diffusivity coefficient of the i-th layer, cm^2/sec; T_i, temperature of the i-th layer, °C; T_0, thermostat temperature, °C; T_f, paraffin premelting temperature, °C; l_i, thickness of the i-th layer, μm; l, thickness of the whole film, μm; ξ, a dimensionless coordinate; τ, dimensionless time; u_i, dimensionless temperature; $\bar{Q}$, dimensionless heat flux; Q_{lim}, limit heating pulse intensity for which the system emerges into the stationary temperature regime, W/cm^2; K, heat-conduction coefficient of the total paraffin and Lavsan layer, W/cm^2; $\varkappa$, thermal diffusivity coefficient of the total paraffin and Lavsan layer, cm^2/sec; l, total thickness of the layers of paraffin and the substrate, cm. Subscripts i = 1 corresponds to the first layer $[0, x_1]$; i = 2 to the second layer $[x_1, x_2]$; i = 3 to the third layer $[x_2, x_3]$; p, for particles; and m for the paraffin medium.

LITERATURE CITED

1. Ya. A. Monosov, "Reversible heterogeneous medium for image recording, based on filler regrouping," Preprint No. 13(296) [in Russian], Inst. Radio Eng. Electronics, USSR Acad. Sci., Moscow (1980).
2. Physics and Chemistry of the Solid State of Organic Compounds [Russian translation], Mir, Moscow (1967).
3. A. F. Chudnovskii, Heat Transfer in Disperse Media [in Russian], GITTL, Moscow (1954).
4. I. G. Portnov, "Problem on the destruction and melting with a jump change in the density taken into account," Heat and Mass Transfer [in Russian], Vol. 2, Nauka i Tekhnika, Minsk (1968), pp. 75-84.
5. W. S. Dorn and D. D. McCracken, Numerical Methods with Fortran IV Case Studies, Wiley (1972).
6. H. S. Carslaw and J. C. Jaeger, Conduction of Heat in Solids, Oxford Univ. Press (1959).

HEAT FORMATION IN A VISCOELASTIC RECTANGULAR PRISM UNDER FORCED HARMONIC OSCILLATIONS

B. P. Gumenyuk

UDC 539.376:536.2.02

The heat formation in a viscoelastic harmonically excited prism that occurs because of mechanical energy dissipation is investigated.

The extensive application of viscoelastic materials in modern engineering arouses considerable interest in the investigation of the thermomechanical behavior of viscoelastic bodies. These materials possess low heat conductivity, a capacity to dissipate mechanical energy, and a temperature dependence of the physicomechanical and strength characteristics. Interaction of the strain and temperature fields is manifested most clearly under continued harmonic deformation. A substantial rise in temperature of the oscillating body is possible here, which occurs because of mechanical energy dissipation. According to some experimental results [1-3], even in the quasistatic frequency domain the heating can influence the longevity of structural elements decisively under definite conditions. In the dynamic frequency range, the level of heat formation rises significantly in the neighborhood of resonances, and it acquires a still more important role [4, 5].

On the basis of the exact solution of the plane dynamic problem of viscoelasticity obtained in [6], heat formation in a viscoelastic prism subjected to harmonic excitation is investigated in this paper. The complex viscoelastic shear modulus is considered frequency-dependent and temperature-independent. An infinitely long prism of rectangular section $|\xi| \leq L$, $|\eta| \leq H$ is considered, which performs forced harmonic tension–compression oscillations under the action of a normal load applied to two opposite faces $\eta = \pm H$. Harmonic displacements with amplitude $u_0 = L\alpha_0$ are given on these faces in solving the dynamics problem [6]. Convective heat transfer is realized between the prism faces and the environment of

Institute of Mechanics, Academy of Sciences of the Ukrainian SSR, Kiev. Translated from Inzhenerno-Fizicheskii Zhurnal, Vol. 47, No. 2, pp. 326-331, August, 1984. Original article submitted March 14, 1983.

temperature T_0 that agrees with the initial temperature of the prism. The dissipative function is taken equal to the mechanical power averaged over the oscillation cycle

$$D = \frac{\omega}{2\pi} \int\limits_{t}^{t+2\pi/\omega} \mathrm{Re}\, \tilde{\sigma}_{jk}\, \mathrm{Re}\, \frac{\partial \tilde{\varepsilon}_{jk}}{\partial t'}\, dt',$$

where $\tilde{\sigma}_{jk} = \sigma_{jk}(\xi, \eta)\exp i\omega t'$, $\tilde{\varepsilon}_{jk} = \varepsilon_{jk}(\xi, \eta)\exp i\omega t'$.

The slow temperature rise in time permits neglecting the influence of the rapidly damped mechanical transient and introducing the temperature $T = \frac{\omega}{2\pi} \int\limits_{t}^{t+2\pi/\omega} T(t')\, dt'$ averaged over the oscillation cycle. The temperature field of prism heating is described by the heat-conduction equation averaged over the oscillation cycle

$$\frac{1}{a}\frac{\partial T}{\partial t} = \frac{\partial^2 T}{\partial \xi^2} + \frac{\partial^2 T}{\partial \eta^2} + \frac{D}{\lambda} \quad (-L < \xi < L, \quad -H < \eta < H, \quad t > 0) \tag{1}$$

with the initial and boundary conditions

$$\begin{gathered} T|_{t=0} = T_0, \\ \frac{\partial T}{\partial \xi} \pm \frac{\alpha_1}{\lambda}(T - T_0) = 0 \quad (\xi = \pm L), \\ \frac{\partial T}{\partial \eta} \pm \frac{\alpha_2}{\lambda}(T - T_0) = 0 \quad (\eta = \pm H). \end{gathered} \tag{2}$$

To construct the dissipative function D it is necessary to know the stress–strain state of the prism which is determined because of solving the dynamic problem of viscoelasticity [6]

$$u_{j,kk} + \frac{1}{1-2\nu} u_{k,kj} + \frac{\rho\omega^2 L^2}{G} u_j = 0 \quad (j, \ k = x, \ y), \tag{3}$$

$$\begin{gathered} u_x = 0, \quad u_y = \pm a_0 \quad (y = \pm y_0), \\ \sigma_x = 0, \quad \sigma_{xy} = 0 \quad (x = \pm 1), \end{gathered} \tag{4}$$

where $u_x = u_\xi/L = u_{x1} + iu_{x2}$, $u_y = u_\eta/L = u_{y1} + iu_{y2}$, $U(x, y, t) = u_x(x, y)\exp i\omega t$, $V(x, y, t) = u_y(x, y)\exp i\omega t$, $x = \xi/L$, $y = \eta/L$, $G = G_1(\omega) + iG_2(\omega)$, $y_0 = H/L$.

To solve the boundary-value problem (3)-(4), an approach is used that extends the known method of superposition [7] to the case of linear viscoelasticity. The technique for constructing the solution is elucidated in [6]. Consequently, the displacement and stress fields are determined.

After having determined the dissipative function D, taking symmetry conditions into account the boundary-value problem (1), (2) takes the following form in dimensionless coordinates

$$\frac{\partial \psi}{\partial \tau} = \frac{\partial^2 \psi}{\partial x^2} + \frac{\partial^2 \psi}{\partial y^2} + F \quad (0 < x < 1, \ 0 < y < y_0, \ \tau > 0), \tag{5}$$

$$\begin{gathered} \psi|_{\tau=0} = 0, \\ \left.\frac{\partial \psi}{\partial x}\right|_{x=0} = 0, \quad \frac{\partial \psi}{\partial x} + B_1\psi = 0, \quad x = 1, \\ \left.\frac{\partial \psi}{\partial y}\right|_{y=0} = 0, \quad \frac{\partial \psi}{\partial y} + B_2\psi = 0, \quad y = y_0, \end{gathered} \tag{6}$$

where

$$\psi = \frac{T - T_0}{a_0^2 T_2}; \quad \tau = \frac{at}{L^2}; \quad T_2 = T_0 - T_r; \quad F = \frac{L^2}{a_0^2 \lambda T_2} D;$$

$$D = \frac{\omega G_0^2 \delta a_0^2}{G_1(1+\delta^2)} [(1-\nu)(s_{x1}^2 + s_{x2}^2 + s_{y1}^2 + s_{y2}^2) - 2\nu(s_{x1}s_{y1} + s_{x2}s_{y2}) + 2(s_{xy1}^2 + s_{xy2}^2)];$$

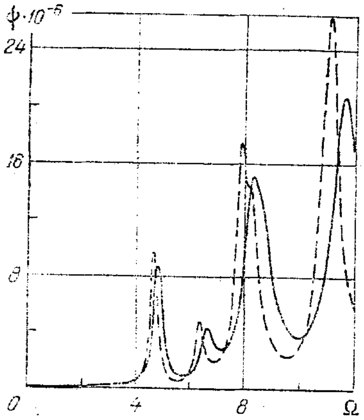

Fig. 1

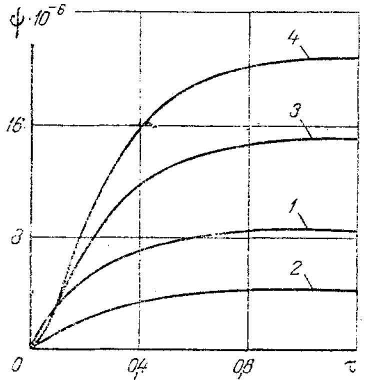

Fig. 2

Fig. 1. Dependence of the dimensionless temperature on the dimensionless frequency for x = 0, y = 0, τ = 1.

Fig. 2. Temperature change with time for x = 0, y = 0.

$$s_x = \sigma_x/2G_0a_0 = s_{x1} + is_{x2}; \quad s_y = \sigma_y/2G_0a_0 = s_{y1} + is_{y2};$$

$$s_{xy} = \sigma_{xy}/2G_0a_0 = s_{xy1} + is_{xy2}; \quad B_{1,2} = \alpha_{1,2}L/\lambda; \quad \delta = G_2/G_1;$$

$$\frac{\sigma_x}{2GB_0} = \nu\cos\gamma y - \sum_{n=1}^{\infty}(-1)^n X_n\left[\frac{(k_n^2+p_2^2)}{4p_1k_n}\frac{\operatorname{ch}p_1x}{\operatorname{sh}p_1} - \right.$$

$$\left. - p_2k_n\frac{\operatorname{ch}p_2x}{\operatorname{sh}p_2}\right]\cos k_ny + y_0\sum_{j=1}^{\infty}(-1)^jY_j\left[\left(\lambda_j^2+\frac{\nu\gamma_0}{2}\right)\frac{\operatorname{ch}q_1y}{\operatorname{ch}q_1y_0} - \lambda_j^2\frac{\operatorname{ch}q_2y}{\operatorname{ch}q_2y_0}\right]\cos\lambda_jx;$$

$$\frac{\sigma_y}{2GB_0} = (1-\nu)\cos\gamma y + \sum_{n=1}^{\infty}(-1)^nX_n\left[\frac{(2k_n^2+\nu\gamma_0)(k_n^2+p_2^2)}{4p_1k_n}\frac{\operatorname{ch}p_1x}{\operatorname{sh}p_1} - \right.$$

$$\left. - p_2k_n\frac{\operatorname{ch}p_2x}{\operatorname{sh}p_2}\right]\cos k_ny - y_0\sum_{j=1}^{\infty}(-1)^jY_j\left[\frac{\lambda_j^2+q_2^2}{2}\frac{\operatorname{ch}q_1y}{\operatorname{ch}q_1y_0} - \lambda_j^2\frac{\operatorname{ch}q_2y}{\operatorname{ch}q_2y_0}\right]\cos\lambda_jx;$$

$$\frac{\sigma_{xy}}{2GB_0} = \sum_{n=1}^{\infty}(-1)^nX_n\frac{k_n^2+p_2^2}{2}\left(\frac{\operatorname{sh}p_1x}{\operatorname{sh}p_1} - \frac{\operatorname{sh}p_2x}{\operatorname{sh}p_2}\right)\sin k_ny +$$

$$+ y_0\sum_{j=1}^{\infty}(-1)^jY_j\lambda_j\left(q_1\frac{\operatorname{sh}q_1y}{\operatorname{ch}q_1y_0} - \frac{q_2^2+\lambda_j^2}{2q_2}\frac{\operatorname{sh}q_2y}{\operatorname{ch}q_2y_0}\right)\sin\lambda_jx;$$

$$\gamma_0 = \gamma_1^2/(1-\nu); \quad \gamma_1^2 = \rho\omega^2L^2/G; \quad \gamma^2 = \gamma_1^2(1-2\nu)/2(1-\nu); \quad p_1^2 = k_n^2 - \gamma^2;$$

$$p_2^2 = k_n^2 - \gamma_1^2; \quad q_1^2 = \lambda_j^2 - \gamma^2; \quad q_2^2 = \lambda_j^2 - \gamma_1^2; \quad k_n = (2n-1)\pi/2y_0; \quad \lambda_j = j\pi;$$

the quantities B_0, X_n, Y_j (n, j = 1, 2, ...) are determined as a result of solving the infinite system of complex linear algebraic equations presented in [6].

Finite differences using an explicit scheme for equations of parabolic type [8] are applies to solve the boundary-value problem (5), (6). To this end, the time spacing $\Delta\tau$ is introduced such that $\tau_k = k\Delta\tau$ (k = 0, 1, 2, ...). The interval $0 \le x \le 1$ is partitioned into N sections of length Δx by the points $x_i = i\Delta x$ (i = 0, 1, ..., N), while the interval $0 \le y \le y_0$ is partitioned into M sections of length Δy by the points $y_j = j\Delta y$ (j = 0, 1, ..., M). Replacement of the derivatives by the appropriate differences results in a difference scheme in $\psi^{k+1}_{i,j}$ with a second-order approximation in the coordinates and a first-order approximation in the time

$$\frac{\psi_{i,j}^{k+1}-\psi_{i,j}^k}{\Delta\tau} = \frac{\psi_{i+1,j}^k - 2\psi_{i,j}^k + \psi_{i-1,j}^k}{\Delta x^2} + \frac{\psi_{i,j+1}^k - 2\psi_{i,j}^k + \psi_{i,j-1}^k}{\Delta y^2} + F_{i,j}^k$$

$$(i = 1, 2, \ldots, N-1; \quad j = 1, 2, \ldots, M-1),$$

$$\psi_{0,j}^{k+1} = \frac{1}{3}(4\psi_{1,j}^{k+1} - \psi_{2,j}^{k+1}), \quad \psi_{N,j}^{k+1} = (4\psi_{N-1,j}^{k+1} - \psi_{N-2,j}^{k+1})/(2B_1\Delta x + 3), \tag{7}$$

$$\psi_{i,0}^{k+1} = \frac{1}{3}(4\psi_{i,1}^{k+1} - \psi_{i,2}^{k+1}), \quad \psi_{i,M}^{k+1} = (4\psi_{i,M-1}^{k+1} - \psi_{i,M-2}^{k+1})/(2B_2\Delta y + 3).$$

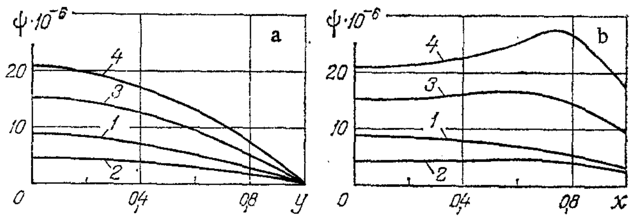

Fig. 3. Temperature distribution along the coordinates for the first four resonances: a) for x = 0; b) for y = 0.

$$\psi_{i,j}^{0} = 0,$$

where $\psi_{i,j}^{k} = \psi(x_i, y_j, \tau_k)$; $F_{i,j}^{k} = F(x_i, y_j, \tau_k)$.

The relationship between Δx, Δy, and $\Delta\tau$ is selected from the stability condition for the difference scheme (7)

$$\Delta\tau \leqslant \frac{1}{2}\left(\frac{1}{\Delta x^2} + \frac{1}{\Delta y^2}\right)^{-1}.$$

Numerical results were obtained for a prism form IRP-1347 rubber [3] for the following data: $G_1 = a_r\omega^b \exp(-2.3b\varphi)$, $\delta = c\omega^d \exp(-2.3d\varphi)$, $\varphi = 8.86T_2/(101.6 + T_2)$, $a_r = 1.35$ MPa, $b = 0.04$, $c = 0.06$, $d = 0.18$, $\nu = 0.5$, $G_0 = 1.18$ MPa, $\rho = 1200$ kg/m³, $T_0 = 20$°C, $T_r = -20$°C, $\lambda = 0.22$ W/m•deg, $c_\varepsilon = 1.86 \cdot 10^6$ J/m³•deg, $B_1 = 4$, $B_2 = 524$, $L = 0.1$ m, $y_0 = 1$.

Curves of $\psi(\Omega)$ are constructed in Fig. 1 for the central point of the prism cross section ($\Omega = \omega L(\rho/G_0)^{1/2}$, $t = 84{,}700$ sec). The solid line corresponds to the general case of a frequency-dependent shear modulus G while the dashes correspond to the case when G is independent of the frequency and is calculated for $\Omega = 1$ ($\omega = 313.6$ sec⁻¹), here $G_1 = 1.35$ MPa and $\delta = 0.06$. As is seen from the results obtained, neglecting the dependence of the material properties on the frequency results in substantial error in the temperature determination, especially at high frequencies. The graphs also illustrate the influence of the dynamic behavior on the heating level of the prism. As should have been expected, the heating intensity at the resonances (local maximums) is considerably higher than in the areas lying nearby. Even for small loading amplitudes, the absolute increment in the temperature reaches a significant value. For instance, for the frequency $\Omega = 0.1$ ($\omega = 31.36$ sec⁻¹) $\psi = 1920$, which corresponds to the value $T - T_0 = 7.68$°C for $u_0 = 1$ mm (here $a_0 = 0.01$, and the deformation is 1%). At higher frequencies, the heating is considerably more intense even for a very much smaller loading amplitudes. Thus, for example, for the frequency $\Omega = 4.8$ (first resonance) $\psi = 8705 \cdot 10^3$ and $T - T_0 = 348$°C for $u_0 = 0.1$ mm ($a_0 = 0.001$, the deformation is 0.1%). Such heating can decisively influence the functional capability of a structural element, in this case a prism.

Curves of $\psi(\tau)$ at the center of the prism cross section are shown in Fig. 2 for the first four resonance frequencies. Curves 1, 2, 3, 4 correspond to the frequency values $\Omega_1 = 4.8$ ($\omega_1 = 1505$ sec⁻¹), $\Omega_2 = 6.6$ ($\omega_2 = 2070$ sec⁻¹), $\Omega_3 = 8.3$ ($\omega_3 = 2603$ sec⁻¹), $\Omega_4 = 11.7$ ($\omega_4 = 3669$ sec⁻¹). As is seen from the figure, at the time $\tau = 1$ the temperature field in the prism is already practically stationary. Therefore, results for the steady-state temperature are presented in Fig. 1. This same remark also refers to the results to be discussed below.

Curves of the dimensionless temperature dependence on the coordinate y are shown in Fig. 3a for the mentioned resonance frequencies for $x = 0$ at the time $\tau = 1$. The maximum of the curves $\psi(y)$ is observed for $y = 0$ (at the central point), which is in agreement with the quasistatic representations in [3]. Analogous resonance distributions of the temperature along the coordinate x for $y = 0$ are shown in Fig. 3b. Here the maximum of the dependence $\psi(x)$ arrives at the point $x = 0$ at the first resonance (curve 1), however, for higher resonances (curves 2-4), the maximum point shifts from the center to the circumference. This is explained by the presence of side motion modes and a substantial nonuniformity in the stress distribution along the coordinate x for resonances higher than the first.

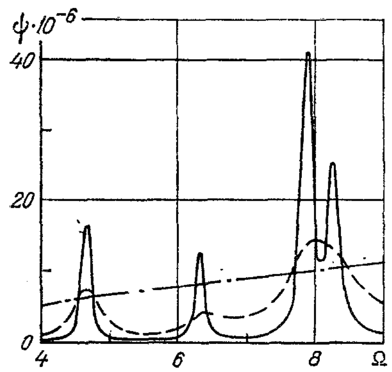

Fig. 4. Dependence of the temperature on the frequency for x = 0, y = 0, τ = 1 for different viscosity levels.

To estimate the influence of viscosity on the heat formation in a prism, the dependence of the temperature on the frequency was investigated at the point x = 0, y = 0, for τ = 1 for different values of δ. The results are shown in Fig. 4, where δ = 0.02 corresponds to the solid line, δ = 0.1 to the dashes, and δ = 1 to the dash-dot line. To eliminate the influence of the frequency dependence of the shear modulus on the results being obtained, it was assumed that $G_1(\Omega) = G_1(1) = 1.35$ MPa.

Therefore, the results represented are qualitative in nature. It is seen from the figure that as the viscosity increases, the resonance values of the temperature diminish, certain resonance vanish, and finally, the curve of the dependence of the temperature on the frequency becomes completely smooth.

NOTATION

U, V, complex displacement; u_ξ, u_η, complex displacement amplitudes; σ_{ij}, ε_{ij}, complex stress and strain amplitudes; ξ, η, Cartesian rectangular coordinates; x, y, dimensionless coordinates; t, τ, physical and dimensionless times; L, H, width and height of the prism cross section; u_0, a given displacement amplitude; T, T_0, average temperature over a cycle and the initial temperature; D, dissipative function; λ, a, $\alpha_{1,2}$, heat conduction, thermal diffusivity, and heat elimination coefficients; c_ε, volume specific heat; ω, Ω, circular and dimensionless frequencies; ψ, dimensionless temperature; ρ, density of the material; ν, Poisson ratio; $G = G_1 + iG_2$, complex shear modulus; G_0, static shear modulus of the material; and a_r, b, c, d, T_r, material constants.

LITERATURE CITED

1. J. Constable, J. G. Williams, and D. J. Burns, "Fatigue and cyclic thermal softening of thermoplastics," J. Mech. Eng. Sci., 12, No. 1, 20-29 (1970).
2. V. G. Karnaukhov, G. A. Yakovlev, and L. P. Goncharov, "Investigation of self-heating of viscoelastic materials under cyclic loads," Probl. Prochn., No. 2, 36-39 (1975).
3. B. M. Gorelik, L. P. Goncharov, V. G. Karnaukhov, et al., "Experimental-theoretical investigation of heat formation in a short viscoelastic cylinder under cyclic compression," Probl. Prochn., No. 1, 68-70 (1977).
4. B. P. Gumenyuk and V. G. Karnaukhov, "On the dynamic behavior of viscoelastic bodies under harmonic excitation," Prikl. Mekh., 16, No. 7, 89-95 (1980).
5. B. P. Gumenyuk, V. G. Karnaukhov, and I. K. Senchenkov, "Influence of thermomechanical affinity on the dynamic behavior of viscoelastic bodies," Zh. Prikl. Mekh. Tekh. Fiz., No. 3, 148-155 (1980).
6. I. K. Senchenkov and B. P. Gumenyuk, "On forced oscillations of a rectangular viscoelastic prism under kinematic excitation," Dokl. Akad. Nauk Ukr. SSR, Ser. A, No. 10, 55-58 (1980).
7. V. T. Grinchenko, Equilibrium and Steady Vibrations of Finite Elastic Bodies [in Russian], Naukova Dumka, Kiev (1978).
8. A. A. Samarskii, Introduction to the Theory of Difference Schemes [in Russian], Nauka, Moscow (1971).